Charge inversion of colloidal particles in an aqueous solution: Screening by multivalent ions

Takamichi Terao and Tsuneyoshi Nakayama
Department of Applied Physics, Hokkaido University, Sapporo 060-8628, Japan
(Received 25 October 2000; published 19 March 2001)

We investigate the structure of the electric double layer on charged colloids by Monte Carlo simulations. Using the primitive model of asymmetric electrolytes, the integrated charge distribution function on a spherical colloidal particle are also studied. With high concentrations of divalent ions, numerical results predict *charge oscillation* and *charge inversion* phenomena, which the traditional Derjaguin-Landau-Verwey-Overbeek theory cannot reproduce.

DOI: 10.1103/PhysRevE.63.041401 PACS number(s): 82.70.Dd, 82.70.Kj, 61.20.Ja

I. INTRODUCTION

Electrostatic interaction plays an important role in aqueous solutions of colloids and polyelectrolytes [1–5]. While the bare Coulomb interaction between charged colloidal particles is purely repulsive, the problem is nontrivial by the presence of the microscopic counterions, which are dispersed in an aqueous solution and screen the direct Coulomb repulsion. For weak Coulomb interaction or high dilution of the macroions, the linearized screening theory of Debye and Hückel always leads to an effective pure-repulsive interaction between macroions. This phenomena is described by the Derjaguin-Landau-Verwey-Overbeek (DLVO) theory, which predicts the screened Coulomb repulsion between charged colloidal particles in an aqueous solution. In the DLVO theory, the effective interaction between particles $U_{\mathrm{DLVO}}(r)$ is given by

$$U_{\mathrm{DLVO}}(r)=\frac{Z^2e^2}{4\pi\epsilon}\left(\frac{e^{\kappa a}}{1+\kappa a}\right)^2\frac{e^{-\kappa r}}{r}, \tag{1}$$

where Z, e, κ, a, ϵ, and r denote the surface charge of colloidal particles (macroions), the elementary charge of an electron, the inverse of Debye-Hückel screening length, a radius of colloidal particles, the dielectric coefficient of the medium, and the center-to-center distance between two colloidal particles, respectively. The inverse screening length κ is given by

$$\kappa^2=4\pi\lambda_B\sum_j n_jq_j^2, \tag{2}$$

where $\lambda_B=e^2/4\pi\epsilon k_BT$ is the Bjerrum length and n_j is the q_j-valent ion density. In general, the interaction between colloidal particles is of importance to determine the physical properties of various colloidal systems [6–11].

Recently, a lot of works have been devoted to clarifying the counterion condensation and the attractive interaction between charged colloids, which are inconsistent with the DLVO theory [3,12–29]. Neu [30] and Sader and Chan [31] have proved analytically that the nonlinear Poisson-Boltzmann equation can only yield repulsion and the numerical result by Bowen and Sharif [32] is not correct. These results have suggested that the attractive interaction between like-charged colloids in an aqueous solution is an essentially fluctuation-based phenomenon, where the effect of fluctuations is neglected in the theoretical treatment based on the Poisson-Boltzmann equation [1,30,31]. In this paper, nonlinear screening effect of charged colloids and their *non-DLVO* behavior are numerically investigated. We perform ''ion-counting'' analysis by Monte Carlo simulation and clarify microion density profiles on a charged colloidal particle. With multivalent salt ions, the calculated results on the electric double layer obey the drastically different profile from that described by the Gouy-Chapman theory [1]. We also confirm that the charge inversion phenomena becomes enhanced with increasing concentrations of multivalent salt ions.

This paper is organized as follows. In Sec. II, we describe the primitive model of colloidal particles in an aqueous solution. In Sec. III, the numerical results on the density profile of microions and the integrated charge distribution function are shown. Section IV is devoted to discussions and conclusions.

II. MODELS

We adopt the primitive model of strongly asymmetric electrolytes to describe the colloidal suspension in an aqueous solution, involving the excluded volume and the Coulomb interaction of negatively charged colloidal particles as well as microions [12,15,33]. Within the primitive model, the discrete structure of the solvent is neglected and the solvent enters into the model by its dielectric constant ϵ, which reduces the Coulomb interaction. The linear system size in x, y, and z directions are taken to be L $(-L/2\leqslant x,y,z\leqslant L/2)$. We consider a spherical macroion with the surface charge $-Ze$ $(Z>0)$ and the diameter d. This macroion is placed on the center of the cubic box, and Z monovalent counterions are fully taken into account. The position of a macroion is fixed and not moved in the simulation. In addition, N salt ions are randomly disposed in a cubic box. The pair potential $V_{mn}(r)$ between m and n is as follows: the interaction between a macroion m and a microion n is given by

$$V_{mn}(r)=\begin{cases}\infty & \text{for} \quad r\leqslant d/2+r_0\\ -Zq_ne^2/4\pi\epsilon r & \text{for} \quad r>d/2+r_0\end{cases}, \tag{3}$$

and the interaction between microions m and n is given by

TABLE I. Parameters for the runs A, B, C, D, E, and F.

Run	c (M)	Valence of microions	d (nm)	L (nm)
A	0.09	2:2	4.0	24.0
B	0.72	2:2	2.5	12.0
C	1.25	2:2	2.0	10.0
D	2.4	2:2	2.0	8.0
E	2.4	2:1	2.0	8.0
F	1.25	1:1	2.0	10.0

$$V_{mn}(r)=\begin{cases}\infty & \text{for} \quad r\leqslant 2r_0 \\ q_m q_n e^2/4\pi\epsilon r & \text{for} \quad r>2r_0\end{cases}, \tag{4}$$

where q_m is the valence of a microion m, and r_0 is the radius of microions. We impose periodic boundary conditions in x, y, and z directions, and consider the condition of global charge neutrality in the system.

III. NUMERICAL RESULTS

In this section, we show the numerical results on the screening effect of charged colloidal particles. The microion density profiles on a negatively charged colloidal particle are studied by Monte Carlo simulation in the (N,V,T) ensemble. We start with an arbitrary microion configuration which does not penetrate into a colloidal particle located at the center of the box. It takes 2×10^4 Monte Carlo steps (MCS) to get the system into equilibrium, and 1×10^5 MCS to take the canonical average after the equilibrium. We also take the sample average over 20 samples for each run. In the following simulation, the temperature T and the relative dielectric constant of water ϵ_r are taken to be $T=300\,\mathrm{K}$ and $\epsilon_r=78$, respectively, and the magnitude of the surface charge on a macroion Z is set to be $Z=20$. The radius of microion core r_0 is taken to be $r_0=2.0\,\text{Å}$, respectively. Assume that in addition to Z monovalent counterions, the system contains N additional salt ions, where the number of added salt ions N is taken to be $N=1500$. Other parameters used in the simulations are displayed in Table I. The system size of the cubic box is determined by the salt concentration c and the number of salt ions N. To treat the periodic boundary condition on long-range Coulomb interaction, we adopt Lekner summation technique instead of the Ewald summation method [34]. For the technical detail of treating periodic image charges, see Ref. [34].

Figure 1 shows the density profile of counterions and added salt ions around a colloidal particle (run A). The system contains 750 divalent cations, 750 divalent anions, and 20 monovalent counterions. The solid line, dashed line, and dotted line denote the density profiles of divalent cations $n_{+2}(r)$, the divalent anions $n_{-2}(r)$, and the monovalent counterions $n_{+1}(r)$, respectively. In Fig. 1, the solid line is monotonically decreasing at $r\geqslant d/2$, and the dashed line is monotonically increasing. From this figure, we can see that (i) the magnitude of $n_{+2}(r)$ and $n_{-2}(r)$ becomes constant as $r\to\infty$, and (ii) the screening length κ^{-1} is sufficiently small compared with the system size of the cubic box. The former

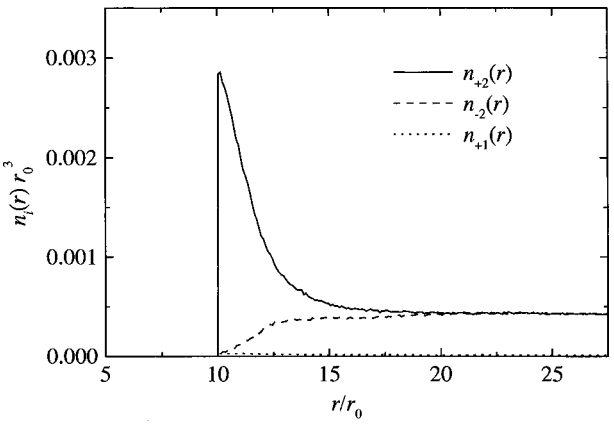

FIG. 1. The microion density profiles $n_i(r)$ for run A. The solid line, dashed line, and dotted line show $n_{+2}(r)$, $n_{-2}(r)$, and $n_{+1}(r)$, respectively.

agrees well with the Guoy-Chapman theory, and the latter indicates that the finite-size effects are not relevant. Figure 2 shows the integrated charge distribution function $P(r)$ for run A, which is defined to be

$$P(r)\equiv -Z+\sum_i \int_0^r z_i n_i(r) 4\pi r^2 dr, \tag{5}$$

where the valences of microions z_i are given by $z_i=+2$, -2, and -1. In Fig. 2, we can see that $P(r)$ becomes zero as $r\to\infty$, indicating that a charged colloidal particle in an aqueous solution is fully screened at the distance, sufficiently larger than the screening length κ^{-1}.

Nguyen, Grosberg, and Shklovskii have considered the screening phenomena of strongly charged macroions [35–37]. They have predicted that, at larger concentrations of multivalent ions, charged colloids, or polyelectrolytes in an aqueous solution strongly bind so many oppositely charged microions that the sign of the net macroion charge becomes inverted. On the other hand, in the previous theory such as Debye-Hückel approximation, the simplest screening atmosphere compensates only a part of the macroion charge and the net macroion charge preserves signs of its bare charge.

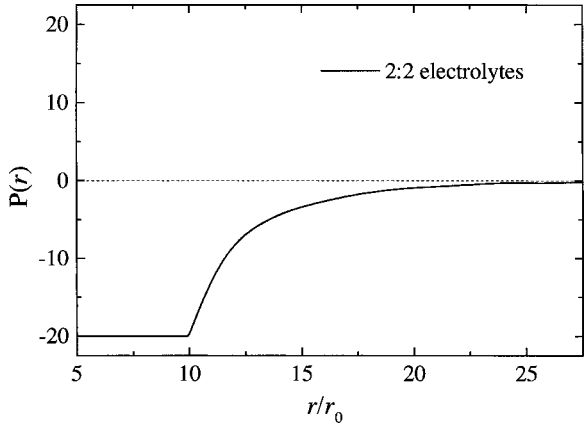

FIG. 2. The integrated charge distribution function $P(r)$ for run A.

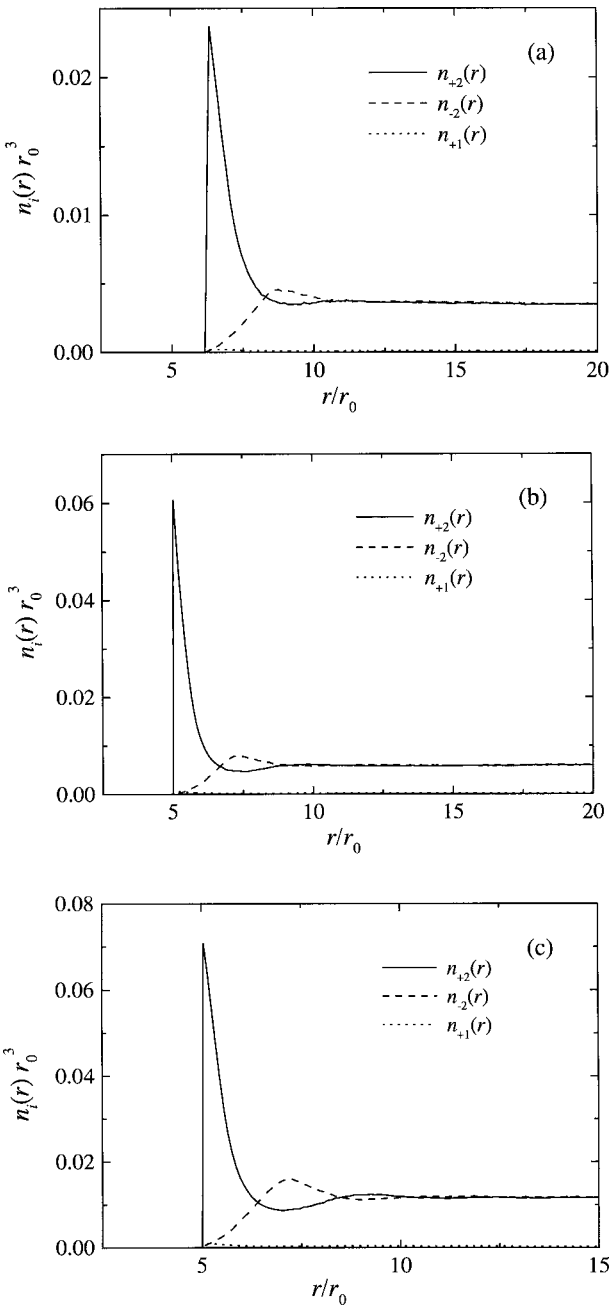

FIG. 3. (a) The microion density profiles $n_i(r)$ for run B. The solid line, dashed line, and dotted line show $n_{+2}(r)$, $n_{-2}(r)$, and $n_{+1}(r)$, respectively. (b) Run C. (c) Run D.

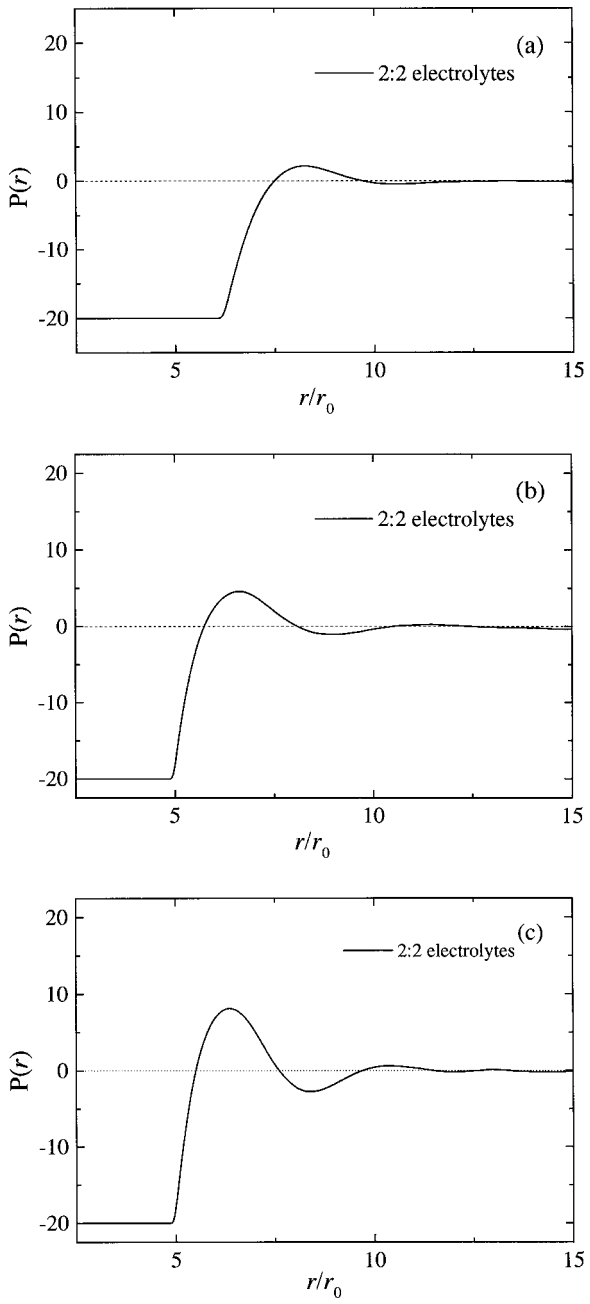

FIG. 4. (a) The integrated charge distribution function $P(r)$ for run B. (b) Run C. (c) Run D.

This phenomena can be thought of as an overscreening effect [38–42]. The details of such charge inversion phenomena are of great interest to clarify the physical properties which cannot be explained by previous theories, for example, attraction between like-charged colloidal particles or polyelectrolytes. In the following, we investigate numerically the existence of charge inversion on spherical colloidal particles in an aqueous solution.

Figure 3 shows the calculated density profiles of microions with larger concentrations of multivalent salt ions. Figures 3(a)–(c) display the results of the density profiles $n_i(r)$ for run B, run C, and run D, respectively. In Fig. 3, there is an apparent difference from Fig. 1, where the density of multivalent cations $n_{+2}(r)$ and that of multivalent anions $n_{-2}(r)$ are oscillating. In addition, there is a range of distance r at which the microion atmosphere is locally negatively charged such as $n_{+2}(r)<n_{-2}(r)$, i.e., with the same sign of charges as the colloidal particle. We can also see that such charge oscillation phenomena becomes enhanced as the concentration of added salt ions c becomes larger. Figure 4 shows the integrated charge distribution function $P(r)$ with the same parameters in Fig. 3. The profile of $P(r)$ overshoots unity, showing a charge inversion at these distances. where the simple PB prediction is clearly incorrect. We also observe the microion density profiles with different valence

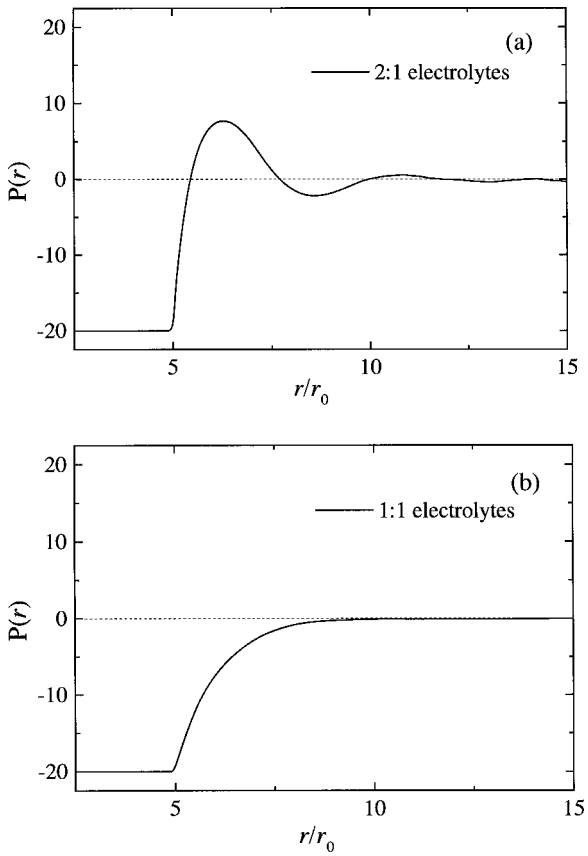

FIG. 5. (a) The integrated charge distribution function $P(r)$ with 2:1 electrolytes (run E). (b) The integrated charge distribution function $P(r)$ with 1:1 electrolytes (run B).

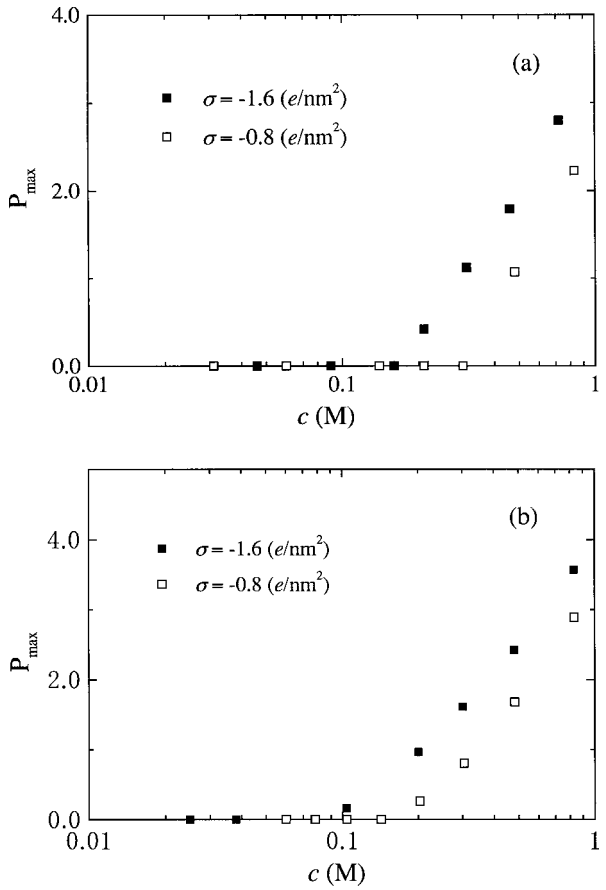

FIG. 6. (a) The maximum value $P_{\max}$ of the integrated charge distribution function with 2:2 added salt ions. Solid squares and open squares show the results with surface charge densities of a macroion $\sigma=-1.6(e/\mathrm{nm}^2)$ and $-0.8(e/\mathrm{nm}^2)$, respectively. (b) The maximum value $P_{\max}$ of the integrated charge distribution function with 2:1 added salt ions. Solid squares and open squares show the results with surface charge densities $\sigma=-1.6(e/\mathrm{nm}^2)$ and $-0.8(e/\mathrm{nm}^2)$, respectively.

in Fig. 5. Figures 5(a) and (b) show the integrated charge distribution function $P(r)$ with 2:1 and 1:1 added salt ions, respectively. Figure 5(b) shows that there is no characteristic charge inversion with monovalent salt ions [43].

Figure 6 shows the maximum value $P_{\max}$ of the integrated charge distribution function $P(r)$ with various different salt concentrations c. In general, $P_{\max}$ becomes zero when the charge inversion does not occur. On the other hand, $P_{\max}$ takes positive values if charge inversion occurs. In Fig. 6, we consider two different surface charge density σ of a macroion. Solid squares and open squares show the results with the surface charge density $\sigma=-1.6\ (e/\mathrm{nm}^2)$ and $-0.8\ (e/\mathrm{nm}^2)$, respectively. Figures 6(a) and (b) denote the results with 2:2 and 2:1 additional salt ions, respectively. In Fig. 6, we find that the maximum value of $P(r)$ deviates from zero and takes a positive value, as the concentration of added salt ions c becomes large.

Rouzina and Bloomfield have theoretically analyzed the attraction between like-charged planer surfaces at a short separation [3]. Linse and Lobaskin have applied their theory into a spherical geometry, and proposed a criterion that the attraction can happen when the coupling parameter Γ obeys $\Gamma\approx 2$ or larger [12]. Here the coupling parameter Γ is defined to be

$$\Gamma\equiv\left(\frac{Z}{4\pi q}\right)^{1/2}\frac{q^2\lambda_b}{d/2+r_0}. \tag{6}$$

They have studied asymmetric electrolytes consisting of highly charged spherical macroions and microions by computer simulations [12,13]. These studies have demonstrated that the effective interaction between colloidal particles becomes repulsive at weak electrostatic coupling, and on the other hand, the attractive force dominates between them at stronger electrostatic coupling [12–14,16,33]. These results are not consistent with the mean-field DLVO theory, which predicts a purely repulsive electrostatic force between like-charged colloidal particles. The main reason of such discrepancy is that the Poisson-Boltzmann equation neglects ion-ion correlations and fluctuation effects. In regard to the electric double layer of charged colloids, we confirm that in the theoretical treatment the continuum mean-field approximation [30–32] is not appropriate to describe this problem, but the primitive-model approach including the ion-ion correlation and the fluctuation effect is required.

IV. CONCLUSIONS

In conclusion, charge inversion phenomena of a colloidal particle are numerically investigated. We have clarified the

microion density profile on a charged colloidal particle $n_i(r)$ and the integrated charge distribution function $P(r)$ by Monte Carlo simulation. The calculated results have shown that the density profiles of multivalent salt ions contradict with the prediction by the Gouy-Chapman theory. Especially, charge oscillation and charge inversion have been confirmed where the net charge of a macroion inverts its sign. These results have confirmed the theoretical prediction in Refs. [35] and [36], where charge inversion can occur on a spherical colloidal particle with multivalent microions. It is expected that these phenomena will be observed directly by electrophoresis experiments.

A correct description of the nonlinear screening effect is very important in order to understand the physical properties of soft matter, such as colloidal suspensions, lipid membranes, and biological polyelectrolytes. From recent studies, it has been suggested that multivalent counterions are condensed and form a two-dimensional strongly correlated liquid at the surface of a macroion [35]. Deserno, Holm, and May have performed molecular dynamics simulations and studied the counterion condensation in a solution of highly charged rigid polyelectrolytes [44]. They have indicated that while the agreement between the Poisson-Boltzmann theory and simulation is excellent in the monovalent, weakly charged case, it deteriorates with the increasing strength of electrostatic interaction and, in particular, the increasing valence of microions. Our numerical results have shown the importance of the ion-ion correlation and fluctuation effects on spherical colloidal system with strong electrostatic couplings, which are neglected in the mean-field theory.

Note that such charge oscillation phenomena will have prounounced effects on the interaction between charged colloids. In the framework of DLVO theory, charged colloidal particles are surrounded by oppositely charged counterions and the overlap of the counterion atmosphere produces repulsive interaction between like-charged colloidal particles. Our results have indicated that the above picture does not hold any more when the concentration of multivalent salt ions is sufficiently high, because the microion density profile on the electric double layer becomes drastically different from that described in the traditional DLVO theory [for example, see Fig. 3(c)]. In addition, we mention recent studies in regard to the association of rodlike *fd*-virus particles by multivalent ions [25]. It is highly possible that such association of rodlike colloids is caused by the anomalous behavior of the electric double layer, adding a sufficiently large amount of multivalent salts. These results will shed light on the microscopic origin of fluctuation-induced attraction between polyelectrolytes [24,45,46].

ACKNOWLEDGMENTS

This work was supported in part by a Grant-in-Aid from the Japan Ministry of Education, Science, and Culture for Scientific Research. The authors thank the Supercomputer Center, Institute of Solid State Physics, University of Tokyo for the use of the facilities.

[1] J. Israelachvili, *Intermolecular and Surface Forces*, 2nd ed. (Academic, London, 1992), and references therein.
[2] S. Alexander, P. M. Chaikin, P. Grant, G. J. Morales, P. Pincus, and D. Hone, J. Chem. Phys. **80**, 5776 (1984).
[3] I. Rouzina and V. A. Bloomfield, J. Phys. Chem. **100**, 9977 (1996).
[4] R. Podgornik and V. A. Parsegian, Phys. Rev. Lett. **80**, 1560 (1998).
[5] H. Aranda-Espinoza, Y. Chen, N. Dan, T. C. Lubensky, P. Nelson, L. Ramos, and D. A. Weitz, Science **285**, 394 (1999).
[6] T. Terao and T. Nakayama, Phys. Rev. E **58**, 3490 (1998).
[7] T. Terao and T. Nakayama, J. Phys.: Condens. Matter **11**, 7071 (1999).
[8] D. G. Grier, J. Phys.: Condens. Matter **12**, A85 (2000).
[9] J. Yamanaka, H. Yoshida, T. Koga, N. Ise, and T. Hashimoto, Phys. Rev. Lett. **80**, 5806 (1998).
[10] T. Terao and T. Nakayama, Phys. Rev. E **60**, 7157 (1999).
[11] T. Terao and T. Nakayama, Suppl. Prog. Theor. Phys. **138**, 386 (2000).
[12] P. Linse and V. Lobaskin, J. Chem. Phys. **112**, 3917 (2000), and references therein.
[13] P. Linse and V. Lobaskin, Phys. Rev. Lett. **83**, 4208 (1999).
[14] N. Grønbech-Jensen, K. M. Beardmore, and P. Pincus, Physica A **261**, 74 (1998).
[15] E. Allahyarov, I. D'Amico, and H. Löwen, Phys. Rev. Lett. **81**, 1334 (1998).
[16] J. Wu, D. Bratka, and J. M. Prausnitz, J. Chem. Phys. **111**, 7084 (1999).
[17] V. Vlachy, Annu. Rev. Phys. Chem. **50**, 145 (1999).
[18] B. Hribar and V. Vlachy, Biophys. J. **78**, 694 (2000).
[19] L. Guldbrand, B. Jönsson, H. Wennerström, and P. Linse, J. Chem. Phys. **80**, 2221 (1984).
[20] R. Kjellander and S. Marčelja, Chem. Phys. Lett. **112**, 49 (1984).
[21] R. Kjellander, T. Akesson, B. Jönsson, and S. Marčelja, J. Chem. Phys. **97**, 1424 (1992).
[22] H. Wennerström, B. Jönsson, and P. Linse, J. Chem. Phys. **76**, 4665 (1982).
[23] J. P. Valleau, R. Ivkov, and G. M. Torrie, J. Chem. Phys. **95**, 520 (1991).
[24] B.-Y. Ha and A. J. Liu, Phys. Rev. Lett. **79**, 1289 (1997); **81**, 1011 (1998).
[25] A. P. Lyubartsev, J. X. Tang, P. A. Janmey, and L. Nordenskiöld, Phys. Rev. Lett. **81**, 5465 (1998).
[26] D. Goulding and J.-P. Hansen, Europhys. Lett. **46**, 407 (1999).
[27] R. R. Netz and H. Orland, Europhys. Lett. **45**, 726 (1999).
[28] Y. Levin, Physica A **265**, 432 (1999).
[29] M. Tokuyama, Phys. Rev. E **59**, R2550 (1999).
[30] J. C. Neu, Phys. Rev. Lett. **82**, 1072 (1999).
[31] J. E. Sader and D. Y. C. Chan, J. Colloid Interface Sci. **213**, 268 (1999).
[32] W. R. Bowen and A. O. Sharif, Nature (London) **393**, 663 (1998).

[33] T. Terao and T. Nakayama, J. Phys.: Condens. Matter **12**, 5169 (2000).
[34] J. Lekner, Physica A **176**, 485 (1991).
[35] B. I. Shklovskii, Phys. Rev. E **60**, 5802 (1999).
[36] T. T. Nguyen, A. Yu. Grosberg, and B. I. Shklovskii, J. Chem. Phys. **113**, 1110 (2000).
[37] T. T. Nguyen, A. Yu. Grosberg, and B. I. Shklovskii, Phys. Rev. Lett. **85**, 1568 (2000).
[38] H. Greberg and R. Kjellander, J. Chem. Phys. **108**, 2940 (1998).
[39] V. I. Perel and B. I. Shklovskii, Physica A **274**, 446 (1999).
[40] S. Y. Park, R. F. Bruinsma, and W. M. Gelbart, Europhys. Lett. **46**, 454 (1999).
[41] E. M. Mateescu, C. Jeppesen, and P. Pincus, Europhys. Lett. **46**, 493 (1999).
[42] R. Messina, C. Holm, and K. Kremer, Phys. Rev. Lett. **85**, 872 (2000).
[43] B. Jönsson, H. Wennerström, and B. Halle, J. Phys. Chem. **84**, 2179 (1980).
[44] M. Deserno, C. Holm, and S. May, Macromolecules **33**, 199 (2000).
[45] V. A. Bloomfield, Biopolymers **31**, 1471 (1991).
[46] M. Kardar and R. Golestanian, Rev. Mod. Phys. **71**, 1233 (1999).